ACS Sustainable Chemistry & Engineering

Research Article

Cite This: ACS Sustainable Chem. Eng. 2018, 6, 4321−4329

pubs.acs.org/journal/ascecg

Reclamation and Harmless Treatment of Waste Cathode Ray Tube Phosphors: Novel and Sustainable Design

Xiaofei Yin,[†,‡] Jiamei Yu,[†,‡] Yufeng Wu,*[,†,‡] Xiangmiao Tian,[§] Wei Wang,[†,‡] Yi-Nan Zhang,[∥] and Tieyong Zuo[†,‡]

[†]Institute of Circular Economy, Beijing University of Technology, No. 100, Pingleyuan Street, Chaoyang District, Beijing 100124, P. R. China

[‡]Institute of Beijing-Tianjin-Hebei Green Development, Beijing University of Technology, No. 100, Pingleyuan Street, Chaoyang District, Beijing 100124, P. R. China

[§]School of Environment, Tsinghua University, Hai Dian, Beijing 100084, P. R. China

[∥]Institute of Biomaterials and Biomedical Engineering, University of Toronto, Toronto, Ontario M5S 3G9, Canada

Supporting Information

ABSTRACT: In this paper, we propose a novel and sustainable process for recycling rare earths (REs) and zinc (Zn) simultaneously from waste cathode ray tube (CRT) phosphors. First, 95% of the impurities such as glass cullets and aluminum foils are removed by simple screening. Then, a self-propagating, high-temperature synthesis reaction following a water-leaching process is performed to recycle Zn selectively. The REs are recycled by a combined process of oxidative leaching and ionic-liquid-based extraction. They are then regenerated to form a new Y_2O_3:Eu^{3+} phosphor. By following this green recycling design, the recovery efficiencies of REs and Zn reach 99.5% and 99%, respectively. The negative bivalent sulfur in ZnS and Y_2O_3:Eu^{3+} is converted completely to SO_4^{2-}, which efficiently avoids the secondary pollution. It should also be pointed out that the main recovery processes are all carried out at room temperature, and the "three wastes" emissions are minimized throughout the process. This work is expected to open new avenues for highly efficient, energy-saving, and pollution-reducing recovery processes for waste CRT phosphors.

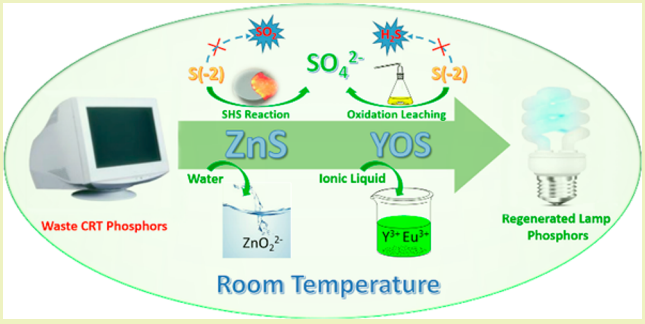

KEYWORDS: *Waste CRT phosphor, Recycling, SHS, Rare earths, Zn, Sustainable design*

INTRODUCTION

Cathodoluminescent phosphors are particularly important luminescent materials in cathode ray tube (CRT) displays. They usually consist of Y_2O_2S:Eu^{3+} (YOS) red phosphor and ZnS-based blue and green phosphors.[1−3] With the rapid development of display technologies such as liquid crystal displays (LCDs), a large number of spent CRTs is being generated every year in both developed and developing countries.[4,5] For instance, approximately 5.96 million units of CRT computer monitors and televisions become obsolete every year in North America.[6] More than 60 million units were discarded in China in 2013 alone.[7] Approximately 1−7 g of cathodoluminescent phosphors are coated in a certain unit of CRT, in which the rare earths (REs) account for approximately 15% and are considered a potential urban mining resource.[8,9] With the continuing shortage of RE mineral resources,[10,11] recycling, as a sustainable and friendly approach, has become significantly important from the view of economy, resource, and environment. Moreover, in addition to RE elements, there are also other valuable metals such as Zn and toxic heavy metals such as Pb also present in the waste CRT phosphors (WCPs). Previously, the collection and recycling of waste CRTs focused largely on the dismantling and the reutilization of the Pb contained in the CRT glass.[12−14] The WCPs were not considered or recycled; rather, they were being discarded, landfilled, or stockpiled as hazardous wastes, causing serious resource waste and environmental pollution. Thus, exploring practical recycling technologies for WCPs cannot be postponed any longer.

Few previous works focused on recycling WCPs, and the overall leaching of both YOS and ZnS was considered to be the most suitable method. Concentrated sulfuric acid could be used to leach REs from waste computer monitor phosphors, but this would cause toxic H_2S to be released directly into the air.[8,15] The synergistic effect of sulfuric acid and hydrogen peroxide proved to be effective for dissolving both Zn and REs, but this method had certain disadvantages such as low Zn leaching efficiency, high energy consumption, and the generation of

Received: December 19, 2017
Revised: February 5, 2018
Published: February 12, 2018

DOI: 10.1021/acssuschemeng.7b04796
ACS Sustainable Chem. Eng. 2018, 6, 4321−4329

complex sulfur-containing products such as elemental sulfur, H_2S, and SO_2.[16] For the recovery of valuable metals from the leaching solutions, sodium sulfide was employed for the selective precipitation of Zn. However, in this case, the coprecipitation of REs was approximately 15−20%, which led to a serious waste of REs.[17] REs could be recycled using the oxalate precipitation method, but the purity of the REs produced was less because of the existence of impurities such as Al, Si, Zn, Ca, and Pb.[17,18]

In summary, all the existing methods adopted the overall leaching of WCPs, followed by recycling the REs and Zn separately. This led to a series of problems, which were mainly reflected in the following five aspects. (I) Pollutant discharge from sulfur: in most of the leaching processes, different toxic gases such as H_2S and SO_2 were released, which caused serious environmental pollution.[15,17] Moreover, the elemental sulfur generated acted as a cladding for the reactants and hindered the leaching reactions.[16] (II) High energy consumption: the leaching processes usually required hours of heating, which increased the energy consumption.[8,17] (III) Neglection of Zn recycling: ZnS, which was one of the main components of WCPs (approximately 60 wt %), was always ignored in the recovery process, resulting in waste. Moreover, the existing methods for recycling Zn were inefficient and required complicated designs.[16,17] Meanwhile, the presence of ZnS increased the difficulty of REs leaching because it also reacted with the acids and slowed down the leaching rate of REs. (IV) Lack of REs regeneration: the purity of the RE oxides obtained by simple precipitation suffered because of impurities such as Al, Ca, Si, and Pb ions, which easily coprecipitated with REs.[18] No research focused on the regeneration and reutilization of REs. (V) Finally, a complete recycling process design for WCPs, under the view of "from waste to product", was lacking.

This work focuses on exploring an efficient and environmental friendly recycling process for REs and Zn from WCPs. First, Zn is recycled separately using an ultrafast, low-cost, and contamination-free self-propagating high-temperature synthesis (SHS) process. Then, the REs are recycled through a combination of oxidative leaching and ionic-liquid (IL)-based extraction. Finally, a new lamp phosphor is regenerated, fulfilling the requirements of value-added reuse. In this work, secondary pollution and energy consumption are controlled strictly during the design of the recovery process. A novel and green recycling process for WCPs is expected to be proposed, which can add important practical value for promoting the efficient recycling of waste RE resources.

EXPERIMENTAL SECTION

Materials and Reagents. All reagents used in this study were of the highest available purity, purchased from the Chemical Reagent Company of Beijing. The pure zinc sulfide (99.99%, Aladdin) and red phosphor ($Y_2O_2S:Eu^{3+}$, LLVCC-R2) were purchased and employed in the process research. The IL used in this study was supplied by Shanghai Chengjie Chemical Co., Ltd. (Shanghai, China). The extraction agent Cyanex272 was purchased from Luoyang Aoda Chemical Co., Ltd. (Luoyang, China). Deionized water (18.2 MΩ.cm) obtained from a Direct-Pure Up 10 water system (RephiLe Bioscience, Ltd.) was used in the experiments, whenever needed. The WCPs used in this study were collected from typical CRTs after dismantling and were supplied by the Changzhou Xiangyu Resource Recycling Technology Co., Ltd. (Changzhou, China).

Analysis Equipment. The concentrations of the REs and other metal irons in the liquid were determined using an inductively coupled plasma optical emission spectrometer (ICP-OES, Optima 8000, PerkinElmer, Shelton, CT). The powder compositions were analyzed by X-ray fluorescence (XRF, PW2403, PANalytical). The infrared images and temperatures of the SHS process were obtained using an Optris PI200 infrared thermal imager (Optris GmbH). The thermogravimetry differential thermal analysis (TG-DTA) data were obtained on a TGA-50 thermogravimetric analyzer (Shimadzu). The mineralogical analysis of samples was carried out in an X-ray diffractometer (XRD) with a Bruker axs D8 Advance using Cu Kα radiation (Bruker, Germany). The morphologies of the samples were examined using a Nova Nano200 scanning electron microscope (SEM, FEI, America). The excitation and emission spectra of phosphors were measured using an F-7000 fluorescence spectrophotometer (Hitachi, Japan).

Methodology. The process described in this article aims to recycle WCPs by employing environmentally friendly and circular economic principles. First, most of the impurities such as Si, Al, and Pb were removed by simple screening. Next, Na_2O_2 and WCP were mixed and ignited to initiate the SHS reaction. The SHS products were treated using deionized water, so that Zn was leached out selectively, enriching the RE content (YOS) in the residues. Third, the REs were leached by oxidative leaching using HCl and H_2O_2 and purified in a IL-based extraction system using [A336][NO_3] and Cyanex272. Finally, a new $Y_2O_3:Eu^{3+}$ phosphor was regenerated through oxalic acid coprecipitation and calcination. During the experiments, we investigated the influences of the main parameters on the recovery efficiencies of REs and Zn and determined the optimum conditions. Details about the experiments are presented in the Section SI.

RESULTS AND DISCUSSION

Pretreatment. The WCP collected from the recycling enterprises are always mixed with impurities such as glass cullet (SiO_2 and PbO), aluminum foils (Al), and dust, etc.[19] In our work, a simple gradation sieving method was employed to remove these impurities, and a series of sieves with different mesh sizes were used (Figure S1a). Figure 1a shows the compositions of the powders at different sieve fractions,

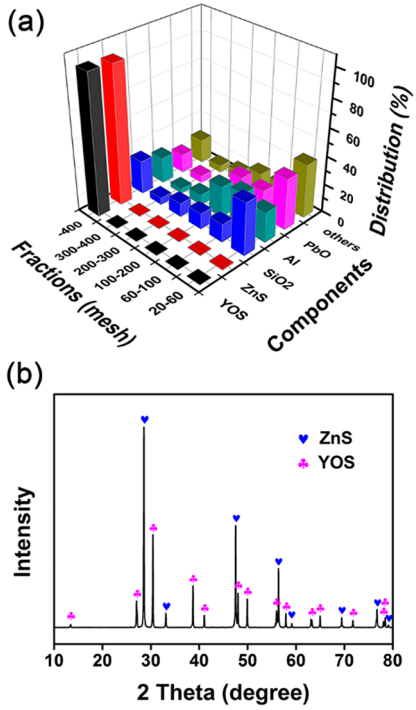

Figure 1. Component analysis of the pretreatment. (a) Distribution of components in WCP at different sieve fractions (wt %). (b) XRD pattern of the PR-WCP.

DOI: 10.1021/acssuschemeng.7b04796
ACS Sustainable Chem. Eng. 2018, 6, 4321−4329

Table 1. Compositions of the PR-WCP

components	YOS	ZnS	SiO_2	PbO	Al	MgO	CaO	Fe_2O_3	Co_3O_4	others
mass %	32.4	61.9	2.41	0.98	1.48	0.232	0.132	0.228	0.167	0.007

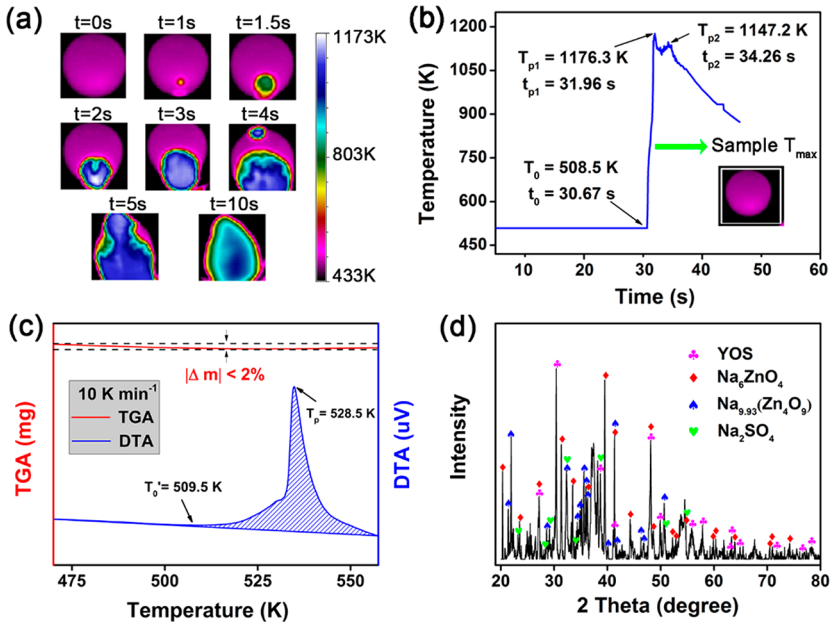

Figure 2. Characteristics of SHS process. (a) Infrared images. (b) Temperature profile by infrared temperature measuring system; (c) TG−DTA curves of SHS process; and (d) XRD pattern of the SHS product.

analyzed using XRF. As can be seen, by screening the WCPs finer, more impurities could be removed. With the use of the 400 mesh, over 76.2%, 86.6%, and 81.2% of SiO_2, Al, and PbO, respectively, were removed. Fortunately, the cathodoluminescent phosphors were collected efficiently, and the loss of YOS and ZnS were less than 0.5% and 1.5%, respectively. The XRD analysis results also demonstrated that the main phases of the pretreated WCP (PR-WCP) were YOS (PDF no. 24-1424) and ZnS (PDF no. 65-9585) (Figure 1b). Table 1 shows the compositions of the PR-WCP analyzed by XRF, which indicates that the cathodoluminescent phosphors were enriched to approximately 95 wt %. The obtained PR-WCP was collected and dried for the subsequent recovery processes. The details about gradation sieving and the mass distribution calculations of the different components at different sieve-fractions are provided in Section SII.

Selective Recovery of Zn. In this section, we report a novel process to recycle Zn selectively from WCP by employing an SHS process. Compared to the traditional methods, SHS has the advantages of excellent energy utilization efficiency, time saving, less environmental pollution, and low-cost facility construction, because, once started, the SHS reactions will continue spontaneously using the heat released, and will be completed in seconds, without requiring any supplemental energy.[20] We innovatively proposed that the SHS reaction could be ignited when ZnS (the main component of WCP) and Na_2O_2 were mixed evenly, and the reaction products were soluble in water. Thus, Zn could be recycled selectively, which not only avoided the interference of ZnS during RE recycling but also increased the overall recovery efficiency of WCPs.

SHS Process. The PR-WCP and Na_2O_2 were mixed uniformly and compacted into a tablet. Then, a heating plate was employed for igniting the samples in order to facilitate the observation. Figure S4 shows the visible phenomena of the SHS process in three different stages: (1) ignition, (2) self-propagation of the combustion wave, and (3) product cooling. We captured infrared thermal images of the SHS reaction (Figure 2a), which illustrated that the entire process took only a few seconds. The spreading speed of the combustion wave was calculated to be approximately 38 mm s^{-1}, which was in the range of the reported typical combustion wave speeds of 1−150 mm s^{-1}.[21] Figure 2b shows the temperature profile of the SHS reaction, obtained using an infrared temperature measuring system, where the temperatures represent the hottest spots of the entire sample during SHS. The maximum temperature reached at surface of the SHS product was 1176.3 K, and the initial heating rate of the SHS process, obtained from Figure 2b, was 518 K s^{-1}. Thermal analysis of the mixture of ZnS and Na_2O_2 was conducted using TG-DTA at a heating rate of 10 K min^{-1} (Figure 2c). The DTA curve showed that the ignition temperature (T_0') was 509.5 K, which was consistent with the results by the infrared temperature measurement (T_0 = 508.5 K). After reaching the ignition temperature, a sharp exothermic peak appeared, which indicated the occurrence of the SHS reaction. The TGA curve showed that the mass change of the mixture was less than 2%, which could be ignored within the margin of error. Thus, we could confirm that no gases (such as SO_2) were generated and that no other substance (such as O_2 or CO_2) was involved in the SHS reaction, except ZnS and Na_2O_2. Figure 2d shows the XRD pattern of the SHS product. Compared to the PR-WCP, the peaks of ZnS disappeared, but those of YOS were still observed. After the SHS reaction, Na_6ZnO_4 (PDF no. 70-2073), $Na_{9.93}Zn_4O_9$ (PDF no. 87-0721), and Na_2SO_4 (PDF no. 86-0803) were generated. The main SHS reaction can be expressed as in eqn 1. It is worth

DOI: 10.1021/acssuschemeng.7b04796
ACS Sustainable Chem. Eng. 2018, 6, 4321−4329

mentioning that, via the SHS process, the divalent sulfur in ZnS was oxidized to Na_2SO_4, rather than to SO_2 or S^0, which corresponded with the results of DTA. Thus, the sulfur pollution caused by the existing acid leaching processes could be avoided completely by following this SHS process.

$$ZnS + 4Na_2O_2 \rightarrow Na_6ZnO_4 + Na_2SO_4 \quad (1)$$

Actually, the SHS reaction could be easily ignited using a lighter (Figure S4), and the samples need not been preheated. The phenomenon of the SHS process shown in Figure S4b also demonstrates that the SHS reaction belongs to point-heating and not synchro-heating.[22−24] Moreover, at such high temperatures as that produced by SHS, the incendive trace impurities such as resin and graphite can be burnt efficiently in air, resulting in the removal of these impurities while avoiding contamination.[23,25]

Water Leaching Process. The products of the SHS process (Na_2SO_4 and Na_6ZnO_4) easily reacted with water at room temperature and dissolved completely in minutes. The reactions can be expressed by eqs 2, 3, and 4. According to the distribution curve of Zn in the system of Zn(II)−H_2O, the species of Zn present in the aqueous alkaline medium with pH > 13 were $Zn(OH)_2^{4-}$ and ZnO_2^{2-}.[26] The pH of the water leaching solution was higher than 14, when tested by a pH-meter. Eq 2 illustrates that an alkaline solution can be produced by the reaction itself, which ensures the solubility of $Zn(OH)_2^{4-}$ and ZnO_2^{2-} in the water leaching solution.

$$Na_6ZnO_4 + 2H_2O \rightarrow ZnO_2^{2-} + 6Na^+ + 4OH^- \quad (2)$$

$$Na_6ZnO_4 + 2H_2O \rightarrow Zn(OH)_4^{2-} + 6Na^+ \quad (3)$$

$$Na_2SO_4 \xrightarrow{H_2O} 2Na^+ + SO_4^{2-} \quad (4)$$

To optimize the separation of Zn, we carried out comparative tests for the SHS reactions in the case of two pretreatment processes: (1) mixing in the form of a powder and (2) compacting the mixture into tablets. The effect of the different mass ratios of Na_2O_2 to WCP on the separating efficiency of Zn is shown in Figure 3a. When the SHS process was conducted on the powder form of the mixture, the leaching rate of Zn could reach 85% at a mass ratio of 3.5, which dropped down at higher ratios. In contrast, when the mixed powders were compacted tightly, the dissolution rate of Zn reached almost 99% at a mass ratio of 3.0 and remained the same at higher ratios. This could be because compacting made the particles contact more fully, which contributed to the sufficient reaction of ZnS in WCP and Na_2O_2.[27] The inset of Figure 3a shows the conversion rate of the sulfur element from S(II) in ZnS to Na_2SO_4, which gives a trend similar to that of the dissolution rate of Zn. At a mass ratio of 3.0, the conversion efficiency of sulfur reached more than 99.5%, which also proved the results of the TGA measurement (Figure 2c). The detection of SO_4^{2-} in the water leaching solution is introduced in Section SIII. After the water leaching of the SHS product, the lixivium containing ZnO_2^{2-} ions was collected by filtering. Then, Zn powder could be regenerated efficiently by simple electrolysis, from the alkaline lixivium.[28−32]

Enrichment of RE Components. After filtration, no REs were detected in the lixivium by ICP-OES, which demonstrated that ZnS was separated efficiently and that YOS was enriched. Figure 3b shows the XRD patterns of the water leaching residues, which illustrates that the main compositions are YOS

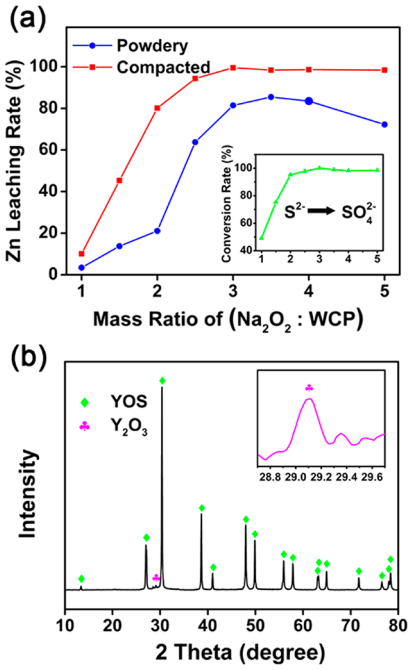

Figure 3. Characteristics of Zn extraction. (a) Effect of mass ratio of Na_2O_2 to WCP on Zn leaching rate. (b) XRD pattern of residues after leaching of the SHS product.

and a small amount of Y_2O_3 (PDF no. 43-1063). The generation of Y_2O_3 could be caused by the instant high temperature and the excess Na_2O_2 during the SHS process, which oxidized small portions of the YOS into Y_2O_3. The chemical composition of the RE residue, named enriched WCP (ER-WCP), analyzed by XRF is shown in Table 2. Compared

Table 2. Composition of ER-WCP

components	YOS	ZnS	SiO_2	PbO	Al	others
mass %	90.21	1.54	0	0.91	0	7.54

with the composition of WCP, the proportion of YOS was enhanced from 32.4% to 90.2%, and ZnS was separated efficiently. Some of the residual aluminum and silicon dioxide were converted to soluble $NaAlO_2$ and Na_2SiO_3 during the SHS process, which could be separated during the water leaching process.[33]

Leaching of REs from ER-WCP. Having separated the ZnS using SHS process, we now describe in detail a simple leaching process for the complete dissolution of REs from the ER-WCP at room temperature. In our work, pure and unmixed phosphors of YOS were employed for the leaching process optimization. In our previous study, it was identified that the mixture of hydrochloric acid (HCl) and hydrogen peroxide (H_2O_2) could be an optimal choice for the efficient leaching of YOS, as shown in Figure S6.[34] Figure 4 (panels a and b) shows the effects of H_2O_2 and HCl concentrations on the leaching efficiency of the YOS at room temperature. The results indicated that the leaching efficiency of REs increased with the increase in the H_2O_2 and HCl concentrations. The time for complete dissolution was reduced from 12 to 6 h when the H_2O_2 and HCl concentrations were increased from 7.5% and 3.0 M to 10% and 4.0 M, respectively.

Figure 5 shows the practical application of the optimum leaching conditions (4 M HCl and 10% H_2O_2) on the real ER-

DOI: 10.1021/acssuschemeng.7b04796
ACS Sustainable Chem. Eng. 2018, 6, 4321−4329

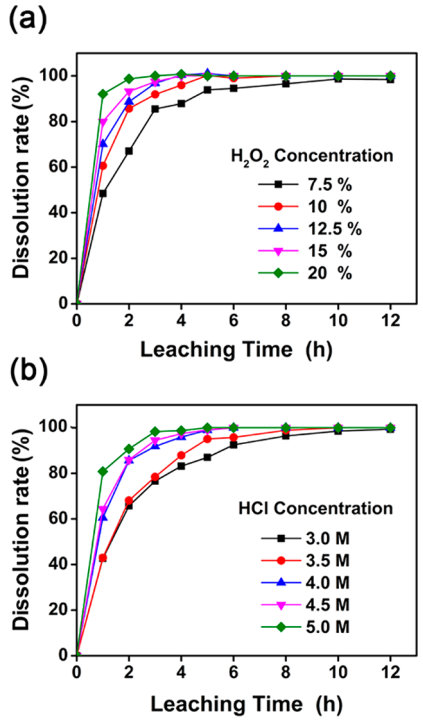

Figure 4. Optimization of RE leaching process. (a) Effects of hydrogen peroxide concentration on RE dissolution. (b) Effects of hydrochloric acid concentration on RE dissolution.

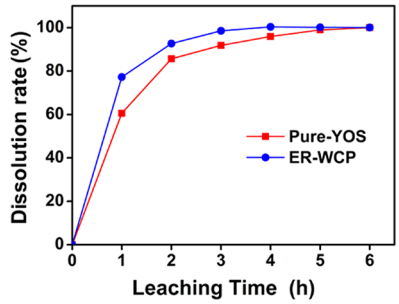

Figure 5. Dissolution of ER-WCP.

WCP. It can be seen that all REs were dissolved after stirring for 4 h. When compared with the leaching result of pure YOS, the presence of Y_2O_3 in ER-WCP indeed caused an increase in the RE leaching rate. On the other hand, no H_2S or SO_2 were detected using lead acetate paper and sulfur dioxide test paper when leaching under the optimal conditions. The XRD analysis of YOS after reacting for 1 h demonstrated that no elemental sulfur was generated (Figure S7). As proof, we found that the negative bivalent sulfur in YOS was oxidized to SO_4^{2-} tested by the barium sulfate precipitation method (eq 5). Thus, the room temperature leaching method of RE was a pollutant-free process using common and cheap chemicals, which had obvious advantages over the existing leaching techniques. Moreover, the generated SO_4^{2-} helped precipitate and separate the Pb^{2+} ions after filtration.

$$(Y, Eu)_2O_2S + 4H^+ + 4H_2O_2 \rightarrow RE^{3+} + 6H_2O + SO_4^{2-} \quad (5)$$

IL-Based Extraction. Solvent (liquid−liquid) extraction has always been one of the most common methods for the separation of RE metals. However, in conventional solvent extraction, the large amounts of volatile organic solvent (VOS) used has been problematic, as they are highly volatile and toxic and they easily pollute the environment.[35] Ionic liquid is a type of burgeoning green alternative to conventional VOSs, owing to their excellent characteristics such as high heat capacity, low vapor pressure, and stable properties.[36,37] In this work, an IL-based extraction system was used to separate the REs from the oxidative leaching solution. We selected tricaprylmethylammonium nitrate ([A336][NO_3]) as the IL because of its significant advantages over imidazolium and pyridine ILs. The extraction of metal ions by [A336][NO_3] is an ion-type mechanism ($[A336]_x[RE]_y$) rather than the ion-exchange, which can avoid the loss of IL components and the pollution caused by other ILs containing fluoride.[38,39]

Figure 6 shows the results of the IL-based extraction process. In the beginning, different organic extractants were used combined with [A336][NO_3] to select an appropriate IL-based extraction system, including neutral organophosphates (TBP, TRPO, Cyanex923, and CA12) and acidic organophosphates (P204, P507, PC88A, and Cyanex272). As shown in Figure 6a, the RE extraction efficiency when using acidic organophosphates were apparently higher than those when using neutral organophosphates. Cyanex272 presented the highest extraction efficiency for both Y and Eu. Considering the extraction efficiencies of other impurities, the system "[A336][NO_3] + Cyanex272" was identified as the optimal extraction system. Figure 6b illustrates the effects of pH on the extraction rates of different metals. At a pH of 2.0, the extraction rates of the metals kept stable even if we continued to increase the pH. The result showed that Co and Mg could be separated completely from the other metals. It was obvious that the extraction rate of Y was higher than that of Eu but lower at pHs over 1.0, which could be because the volume ratio of oil phase/aqueous phase (O/A) was too small to load more Y in the oil phase (Y occupied almost 90% of the total metal ion concentration in the lixivium). Then, we investigated the effects of O/A on the extraction rates of different metals. As shown in Figure 6c, at an O/A of 1.0, the extraction rates of Y, Eu, Zn, Fe, and Ca could reach 99.9%, 99.1%, 99.9%, 99.1%, and 68.1%, respectively, while Co and Mg were still in the aqueous phase. Given the fact that the nitrate ion of HNO_3 contributed to the regeneration [A336][NO_3],[39] 1 mol/L of HNO_3 was used for stripping the REs. As shown in Figure 6d, the stripping rates of Y and Eu increased with the decrease of O/A, and the single extraction efficiency of REs reached 90% at the O/A of 0.1. Thus, the REs could be stripped efficiently into the aqueous phase after 2−3 times of extraction. Satisfyingly, Zn and Fe were left in the oil phase and separated completely from the REs. Although Ca could not be separated completely by the single extraction, it could be removed by the multistage extraction. In conclusion, through the IL-based extraction, impurities such as Mg, Co, Zn, Fe, and Ca could be separated from the REs. The REs solution would be utilized for regenerating a new red phosphor after purification. The IL-based extraction system, after stripping, could be recycled for the next extracting phase.

Regeneration of Y_2O_3:Eu^{3+} Phosphor. Eu^{3+}-activated Y_2O_3 (Y_2O_3:Eu^{3+}) has always been one of the most popular red phosphors and is widely used in fluorescent lamps.[40,41] In this work, we put forward an idea, for the first time, to recycle REs from WCPs and directly regenerate new Y_2O_3:Eu^{3+} red phosphor for fluorescent lamps, which enabled high value reuse of WCPs. After leaching and IL-based extraction, Y and Eu were recycled and purified in the solution with a molar ratio

DOI: 10.1021/acssuschemeng.7b04796
ACS Sustainable Chem. Eng. 2018, 6, 4321−4329

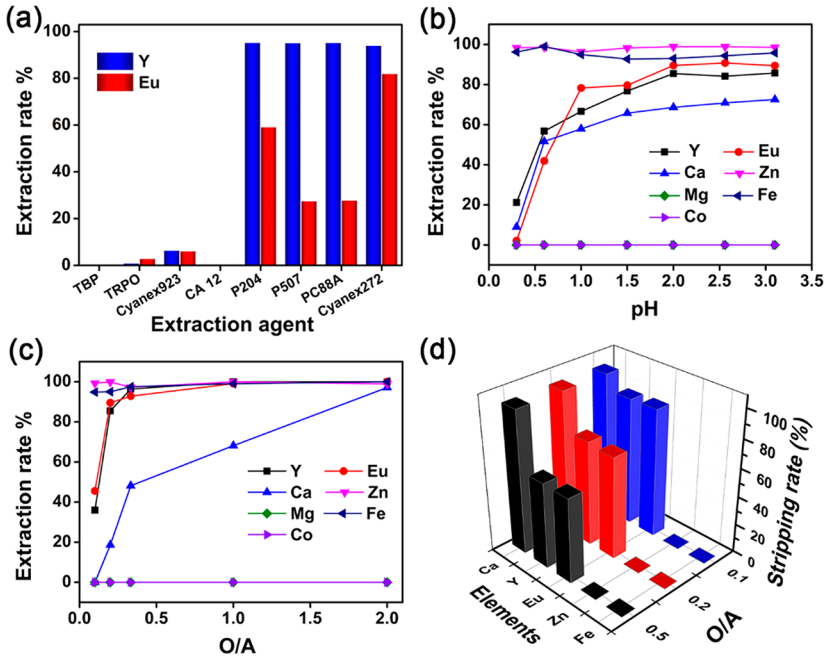

Figure 6. Optimization of IL-based extraction process. (a) Selection of appropriate extraction agents; (b) effects of pH on the extraction rates of different metals; (c) effects of O/A on the extraction rates of different metals; and (d) stripping of REs using an acidic aqueous phase.

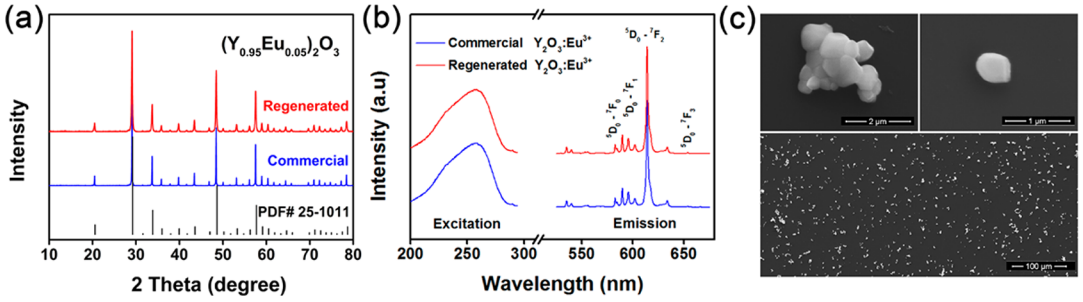

Figure 7. Properties of the regenerated Y_2O_3:Eu^{3+} phosphor. (a) XRD patterns of the regenerated and commercial Y_2O_3:Eu^{3+} phosphor; (b) PL/PLE spectra from regenerated and commercial Y_2O_3:Eu^{3+} phosphor; and (c) SEM images of the regenerated phosphor.

of 19:1 and could be directly used for the preparation of Y_2O_3:Eu^{3+} phosphor.[42,43] Oxalic acid was employed for the precipitation, resulting in >99.5% yield of the $(RE)_2(C_2O_4)_3$ being recycled.[34] Polyethylene glycol (PEG) was dissolved in the RE solution as the surfactant to adjust the morphology of the regenerated Y_2O_3:Eu^{3+} phosphor. The obtained RE oxalates were calcined at 1400 °C to synthesize the regenerated phosphor, which had a purity >99% when analyzed using ICP-OES. Figure 7a compares the XRD patterns of the regenerated and commercial Y_2O_3:Eu^{3+} phosphors. The XRD results were virtually identical with $(Y_{0.95}Eu_{0.05})_2O_3$ (PDF no. 25-1011), which confirms the successful synthesis of Eu^{3+}-doped yttria phosphor. The photoluminescence (PL) and photoluminescence excitation (PLE) spectra of the regenerated phosphors were tested using a fluorescence spectrophotometer and compared with that of the commercial Y_2O_3:Eu^{3+} phosphor. The PL spectra were obtained with an excitation wavelength of 254 nm, and the PLE spectra were obtained at an emission wavelength of 614 nm. The PL/PLE spectra were compared and normalized to the peaks connected with the commercial phosphors luminescence. As shown in Figure 7b, it was obvious that the PL/PLE spectra of the regenerated and commercial phosphors were essentially identical. The broad band with a maximum at ∼254 nm on the excitation spectra could be attributed to the charge transfer process related to the excitation of an electron from the 2p state of O^{2-} to the 4f state of Eu^{3+}, which was why the Y_2O_3:Eu^{3+} phosphor can absorb the ultraviolet radiation by mercury at 253.7 nm.[44,45] The strongest emission peak at 614 nm is due to the forced electric dipole transition of Eu^{3+} ($^5D_0 - {}^7F_2$), resulting in a red emission, which was allowed as the europium ion occupied a site without an inverse center.[41,43] Other peaks corresponding to the $^5D_0$–$^7F_0$ transition at 583 nm, $^5D_0$–$^7F_1$ transition at 590, 595, and 602 nm, and the $^5D_0$–$^7F_3$ transition at 653 nm were also observed.[46−48] The phosphor regenerated from WCP showed a high photoluminescence efficiency when comparing the relative emission intensities (Figure 7b), which reached approximately 98% of that of commercial phosphor. The morphological observation by SEM (Figure 7c) showed that the average particle size of the regenerated phosphor was approximately 500 nm and that the particles were usually aggregated as larger particles in the range of 1−5 μm. The surfaces of the regenerated particles were smooth and presented a near-spherical morphology, which resulted in a larger specific surface area and contributed to the fluorescence performance. When comparing with the SEM micrographs of

DOI: 10.1021/acssuschemeng.7b04796
ACS Sustainable Chem. Eng. 2018, 6, 4321−4329

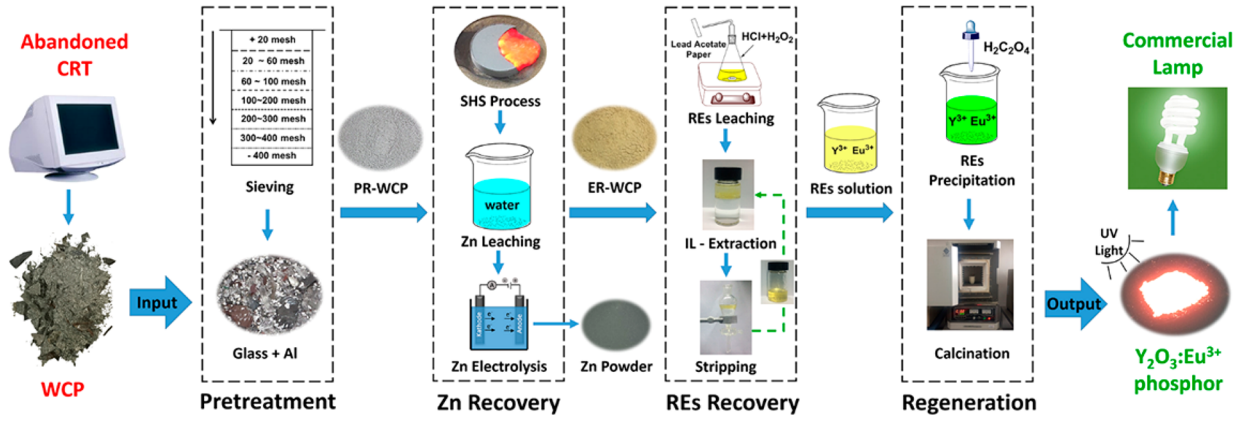

Figure 8. Proposed green process for recovery of WCP.

the commercial Y_2O_3:Eu^{3+} phosphors (Figure S8), the particle size distributions of the commercial phosphors were found to be more uniform, and the agglomerates were more loosely packed, although the single particle size of our regenerated phosphor was smaller (the particle size of the commercial phosphor is approximately 1 μm). That could be the reason why the photoluminescence efficiency of the regenerated phosphor was slightly lower than that of the commercial phosphor. The luminescent properties can be further optimized by adjusting the parameters such as calcination, atomic ratio of Y/Eu, and the addition agents,[40,49,50] which will be investigated in our future work.

Green Recovery Process Design. On the basis of the details, the green recovery process for WCP was proposed as shown in Figure 8. A new strategy combining "pretreatment, recycling Zn by SHS process, RE leaching, IL-based extraction, and regeneration" was designed. The entire process was guided well by the principles of "Circular Economy", which were fully embodied in the following four aspects. (I) The energy consumption was minimized: all recovery processes were conducted at room temperature. (II) The cost was minimized: the chemical reagents used, such as Na_2O_2, HCl, and H_2O_2, were common and cheap in industrial manufacture. Moreover, the IL-based extraction system could be recycled and reused. (III) The secondary pollution was controlled strictly: all S(II) was oxidized to SO_4^{2-}, which completely avoided the generation of sulfur pollution such as H_2S and SO_2. The high temperature produced by SHS could burn the incendive trace impurities such as resin and graphite efficiently and avoid contamination. (IV) The concept of "from waste to product" was achieved: the Zn was recycled as electrolytic Zn powder, and the REs were regenerated to be new red phosphors, which could be applied in fluorescent lamps. Moreover, the glass cullet and Al foil separated by screening could be sent to the relevant enterprises for remanufacturing.

The optimized parameters for recycling 100 g of PR-WCP were used as the basis for a techno−economic analysis. The recovery process consisted of four operations: recycling Zn by SHS, RE leaching, IL-based extraction, and regeneration of new red phosphors. The energy cost (EC) and material cost (MC) for each operation were estimated based on the laboratory apparatus and reagents (Table S2), such as stirrer, muffle, leaching agents, etc. As shown in Figure 9, the main energy cost was in the stage of regeneration, which could be attributed to the calcination for phosphor, and there was no need to provide heat for other operations. The material cost was mainly in the

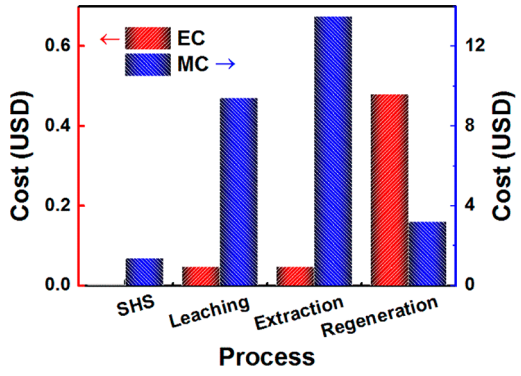

Figure 9. Technical cost analysis.

RE leaching and extraction processes, owing to the high costs of the regents such as HCl and H_2O_2 and the extractants. The total costs of energy and material were computed to be \$0.58 and \$27.48 for recycling 100 g of PR-WCP, which also demonstrated that our recovery design was an energy-saving process. The costs of materials could also be cut down in large industrial production because of the relatively low cost of industrial-grade chemical raw materials when compared to the laboratory ones.

The revenue of the recovery process was assumed to be from two sources: (1) fee charge for disposal of WCP as a hazardous waste and (2) sale of regenerated red phosphor. The fee charge for disposal was only \$0.09, while the regenerated phosphor was worth \$28.83 for recycling 100 g of PR-WCP. However, if it was recycled as pure RE oxides, the value was only \$0.2, according to the 2018 REE prices. Apparently, the high value reuse of WCP as new phosphor can make the plant profitable even without the disposal charge. Thus, the profit from recycling one tonne of PR-WCP was estimated to be \$8600 although this number would be higher if the sale of Zn, Pb, and glass was considered. Nevertheless, the fixed capital costs such as equipment purchase costs, installation costs, and piping costs, etc. were not considered in this research. The calculation details and justification are provided in Section SVII.

CONCLUSIONS

In this work, we proposed a novel and sustainable process for the recovery of REs and Zn from WCP. At the beginning, 95% of the impurities such as glass cullets and aluminum foils were removed by simple screening and the loss of phosphor was less than 1%. Then, it was demonstrated, for the first time, that ZnS

DOI: 10.1021/acssuschemeng.7b04796
ACS Sustainable Chem. Eng. 2018, 6, 4321−4329

could be recycled selectively by employing an ultrafast, low-cost, and environment-friendly SHS process. At the mass ratio of 1:3 for WCP and Na_2O_2, almost 99% of the Zn could be separated by simple water leaching within minutes. Further, the REs in the ER-WCP were recycled by oxidative leaching and IL-based extraction. Experiments showed that the REs could be dissolved completely after stirring in 4 M HCl and 10% H_2O_2 for 4 h, and over 99.5% of the REs could be extracted by the IL extraction system under the conditions of pH = 2.0 and O/A = 1.0. The IL-based extraction system could be reused directly after stripping using dilute HNO_3. Finally, the Y and Eu in the stripped liquid were coprecipitated using oxalic acid and regenerated to form a new Y_2O_3:Eu^{3+} phosphor by simple calcination.

By using the proposed sustainable process, the sulfur pollution observed in the case of the existing technologies could be avoided completely. The recovery was proved to be an energy-saving process employing the principle of room temperature. The comprehensive recovery rate of WCP reached over 98%, and the economic efficiency was maximized through the high-value regeneration of the Y_2O_3:Eu^{3+} phosphor. Therefore, this work paves the way for a highly efficient energy-saving low-cost pollution-reducing industrial process for the efficient and environmentally friendly recovery of WCP.

■ ASSOCIATED CONTENT

Supporting Information

The Supporting Information is available free of charge on the ACS Publications website at DOI: 10.1021/acssuschemeng.7b04796.

Details of the experimental section and screening process, SHS phenomenon and the detection of SO_4^{2-}, selection of appropriate leaching reagents and XRD analysis of YOS after leaching for 1 h, SEM images of the regenerated phosphors, and techno-economic analysis (PDF)

■ AUTHOR INFORMATION

Corresponding Author

*E-mail: wuyufeng3r@126.com. Tel: +86-10-67396234. Fax: +86-10-67396234.

ORCID

Xiaofei Yin: 0000-0002-8665-7884

Yufeng Wu: 0000-0003-2164-4465

Notes

The authors declare no competing financial interest.

■ ACKNOWLEDGMENTS

This research was financially supported by the Beijing Nova Program (Z151100000315014l), the Academician Workstation in the Yunnan Province, Beijing Natural Science Foundation (2182009, 2174067, 2174065), and the Beijing Social Science Fund (no. 17YJA001).

■ REFERENCES

(1) Ozawa, L.; Itoh, M. Cathode Ray Tube Phosphors. *Chem. Rev.* **2003**, *103* (10), 3835−3856.

(2) Thirumalai, J.; Jagannathan, R.; Trivedi, D. C. Y_2O_2S: Eu^{3+} nanocrystals, a strong quantum-confined luminescent system. *J. Lumin.* **2007**, *126* (2), 353−358.

(3) Chen, Y. Y.; Duh, J. G.; Chiou, B. S.; Peng, C. G. Luminescent mechanisms of ZnS: Cu:Cl and ZnS: Cu:Al phosphors. *Thin Solid Films* **2001**, *392* (1), 50−55.

(4) Singh, N.; Li, J.; Zeng, X. An Innovative Method for the Extraction of Metal from Waste Cathode Ray Tubes through a Mechanochemical Process Using 2-[Bis(carboxymethyl)amino]acetic Acid Chelating Reagent. *ACS Sustainable Chem. Eng.* **2016**, *4* (9), 4704−4709.

(5) Fang, W.; Yang, Y.; Xu, Z. PM_{10} and $PM_{2.5}$ and Health Risk Assessment for Heavy Metals in a Typical Factory for Cathode Ray Tube Television Recycling. *Environ. Sci. Technol.* **2013**, *47* (21), 12469−12476.

(6) Yang, Y.; Williams, E. Logistic model-based forecast of sales and generation of obsolete computers in the U.S. *Technol. Forecast. Soc.* **2009**, *76* (8), 1105−1114.

(7) Gong, Y.; Tian, X.; Wu, Y.; Tan, Z.; Lv, L. Recent development of recycling lead from scrap CRTs: A technological review. *Waste Manage.* **2016**, *57*, 176−186.

(8) Resende, L. V.; Morais, C. A. Study of the recovery of rare earth elements from computer monitor scraps - Leaching experiments. *Miner. Eng.* **2010**, *23* (3), 277−280.

(9) Dexpert−Ghys, J.; Regnier, S.; Canac, S.; Beaudette, T.; Guillot, P.; Caillier, B.; Mauricot, R.; Navarro, J.; Sekhri, S. Re-processing CRT phosphors for mercury-free applications. *J. Lumin.* **2009**, *129* (12), 1968−1972.

(10) Bian, Y.; Guo, S.; Jiang, L.; Liu, J.; Tang, K.; Ding, W. Recovery of Rare Earth Elements from NdFeB Magnet by VIM-HMS Method. *ACS Sustainable Chem. Eng.* **2016**, *4* (3), 810−818.

(11) Jin, H.; Park, D. M.; Gupta, M.; Brewer, A. W.; Ho, L.; Singer, S. L.; Bourcier, W. L.; Woods, S.; Reed, D. W.; Lammers, L. N.; Sutherland, J. W.; Jiao, Y. Techno-economic Assessment for Integrating Biosorption into Rare Earth Recovery Process. *ACS Sustainable Chem. Eng.* **2017**, *5* (11), 10148−10155.

(12) Lee, C.; Hsi, C. Recycling of Scrap Cathode Ray Tubes. *Environ. Sci. Technol.* **2002**, *36* (1), 69−75.

(13) Lu, X.; Shih, K.; Liu, C.; Wang, F. Extraction of Metallic Lead from Cathode Ray Tube (CRT) Funnel Glass by Thermal Reduction with Metallic Iron. *Environ. Sci. Technol.* **2013**, *47* (17), 9972−9978.

(14) Zhan, L.; Xu, Z. State-of-the-Art of Recycling E-Wastes by Vacuum Metallurgy Separation. *Environ. Sci. Technol.* **2014**, *48* (24), 14092−14102.

(15) Resende, L. V.; Morais, C. A. Process development for the recovery of europium and yttrium from computer monitor screens. *Miner. Eng.* **2015**, *70*, 217−221.

(16) Tian, X.; Yin, X.; Gong, Y.; Wu, Y.; Tan, Z.; Xu, P. Characterization, recovery potentiality, and evaluation on recycling major metals from waste cathode-ray tube phosphor powder by using sulphuric acid leaching. *J. Cleaner Prod.* **2016**, *135*, 1210−1217.

(17) Innocenzi, V.; De Michelis, I.; Ferella, F.; Beolchini, F.; Kopacek, B.; Vegliò, F. Recovery of yttrium from fluorescent powder of cathode ray tube, CRT: Zn removal by sulphide precipitation. *Waste Manage.* **2013**, *33* (11), 2364−2371.

(18) Innocenzi, V.; De Michelis, I.; Ferella, F.; Vegliò, F. Recovery of yttrium from cathode ray tubes and lamps' fluorescent powders: experimental results and economic simulation. *Waste Manage.* **2013**, *33* (11), 2390−2396.

(19) Hashiba, M.; Hino, T.; Hirohata, Y.; Shinbori, H.; Deyama, S.; Chiyoda, H. Gas desorption and adsorption properties of carbon based material used for cathode ray tube. *Thin Solid Films* **1998**, *332* (1−2), 141−145.

(20) Su, X.; Fu, F.; Yan, Y.; Zheng, G.; Liang, T.; Zhang, Q.; Cheng, X.; Yang, D.; Chi, H.; Tang, X.; Zhang, Q.; Uher, C. Self-propagating high-temperature synthesis for compound thermoelectrics and new criterion for combustion processing. *Nat. Commun.* **2014**, *5*, 4908.

(21) Liang, T.; Su, X.; Tan, X.; Zheng, G.; She, X.; Yan, Y.; Tang, X.; Uher, C. Ultra-fast non-equilibrium synthesis and phase segregation in $In_xSn_{1-x}Te$ thermoelectrics by SHS-PAS processing. *J. Mater. Chem. C* **2015**, *3* (33), 8550−8558.

DOI: 10.1021/acssuschemeng.7b04796
ACS Sustainable Chem. Eng. 2018, 6, 4321−4329

(22) Li, B. Y.; Rong, L. J.; Li, Y. Y.; Gjunter, V. E. Synthesis of porous Ni-Ti shape-memory alloys by self-propagating high-temperature synthesis: reaction mechanism and anisotropy in pore structure. *Acta Mater.* **2000**, *48* (15), 3895−3904.
(23) Merzhanov, A. G. The chemistry of self-propagating high-temperature synthesis. *J. Mater. Chem.* **2004**, *14* (12), 1779−1786.
(24) Fiedler, T.; Belova, I. V.; Broxtermann, S.; Murch, G. E. A thermal analysis on self-propagating high temperature synthesis in joining technology. *Comput. Mater. Sci.* **2012**, *53* (1), 251−257.
(25) Kallio, M.; Ruuskanen, P.; Ki, J. M.; Yli, E. P.; Ki, S. L. H. Use of the Aluminothermic Reaction in the Treatment of Steel Industry By-Products. *J. Mater. Synth. Process.* **2000**, *8* (2), 87−92.
(26) Liu, Q.; Zhao, Y.; Zhao, G. Thermodynamics of Zn(II)-NaOH-H_2O system. *J. Shanghai Univ.* **2010**, *14* (5), 332−336.
(27) Pitt, K.; Sinka, C. Chapter 16 Tableting, In *Handbook of Powder Technology*. Elsevier Science B.V. 2007, *11*, 735−778.
(28) Zhao, Y.; Stanforth, R. Production of Zn powder by alkaline treatment of smithsonite Zn-Pb ores. *Hydrometallurgy* **2000**, *56* (2), 237−249.
(29) St-Pierre, J.; Piron, D. L. Electrowinning of zinc from alkaline solutions at high current densities. *J. Appl. Electrochem.* **1990**, *20* (1), 163−165.
(30) St−Pierre, J.; Piron, D. L. Electrowinning of zinc from alkaline solutions. *J. Appl. Electrochem.* **1986**, *16* (3), 447−456.
(31) Ashtari, P.; Pourghahramani, P. Zinc Extraction from Zinc Plants Residue Using Selective Alkaline Leaching and Electrowinning. *J. Inst. Eng.: Ser. D* **2015**, *96* (2), 179−187.
(32) Liu, Q.; Zhao, Y.; Zhao, G. Production of zinc and lead concentrates from lean oxidized zinc ores by alkaline leaching followed by two-step precipitation using sulfides. *Hydrometallurgy* **2011**, *110* (1−4), 79−84.
(33) Wu, Y.; Wang, B.; Zhang, Q.; Li, R.; Yu, J. A novel process for high efficiency recovery of rare earth metals from waste phosphors using a sodium peroxide system. *RSC Adv.* **2014**, *4* (16), 7927−7932.
(34) Yin, X.; Wu, Y.; Tian, X.; Yu, J.; Zhang, Y.; Zuo, T. Green Recovery of Rare Earths from Waste Cathode Ray Tube Phosphors: Oxidative Leaching and Kinetic Aspects. *ACS Sustainable Chem. Eng.* **2016**, *4*, 7080−7089.
(35) Yang, F.; Kubota, F.; Baba, Y.; Kamiya, N.; Goto, M. Selective extraction and recovery of rare earth metals from phosphor powders in waste fluorescent lamps using an ionic liquid system. *J. Hazard. Mater.* **2013**, *254*, 79−88.
(36) Badruddoza, A. Z. M.; Bhattarai, B.; Suri, R. P. S. Environmentally Friendly *β*-Cyclodextrin−Ionic Liquid Polyurethane-Modified Magnetic Sorbent for the Removal of PFOA, PFOS, and Cr(VI) from Water. *ACS Sustainable Chem. Eng.* **2017**, *5* (10), 9223−9232.
(37) Seitkalieva, M. M.; Kashin, A. S.; Egorova, K. S.; Ananikov, V. P. Ionic Liquids As Tunable Toxicity Storage Media for Sustainable Chemical Waste Management. *ACS Sustainable Chem. Eng.* **2018**, *6* (1), 719−726.
(38) Zhu, M.; Zhao, J.; Li, Y.; Mehio, N.; Qi, Y.; Liu, H.; Dai, S. An ionic liquid-based synergistic extraction strategy for rare earths. *Green Chem.* **2015**, *17* (5), 2981−2993.
(39) Sun, X.; Ji, Y.; Guo, L.; Chen, J.; Li, D. A novel ammonium ionic liquid based extraction strategy for separating scandium from yttrium and lanthanides. *Sep. Purif. Technol.* **2008**, *63*, 61−68.
(40) Kang, Y. C.; Roh, H. S.; Bin Park, S. Preparation of Y_2O_3:Eu phosphor particles of filled morphology at high precursor concentrations by spray pyrolysis. *Adv. Mater.* **2000**, *12* (6), 451.
(41) Wakefield, G.; Holland, E.; Dobson, P. J.; Hutchison, J. L. Luminescence Properties of Nanocrystalline Y_2O_3:Eu. *Adv. Mater.* **2001**, *13* (20), 1557.
(42) Dupont, D.; Binnemans, K. Rare-earth recycling using a functionalized ionic liquid for the selective dissolution and revalorization of Y_2O_3:Eu^{3+} from lamp phosphor waste. *Green Chem.* **2015**, *17* (2), 856−868.
(43) Zhu, Q.; Li, J.; Li, X.; Sun, X. Morphology−dependent crystallization and luminescence behavior of $(Y,Eu)_2O_3$ red phosphors. *Acta Mater.* **2009**, *57* (20), 5975−5985.
(44) Buijs, M.; Meyerink, A.; Blasse, G. Energy transfer between Eu^{3+} ions in a lattice with two different crystallographic sites: Y_2O_3:Eu^{3+}, Gd_2O_3:Eu^{3+} and Eu_2O_3. *J. Lumin.* **1987**, *37* (1), 9−20.
(45) Avdeev, S. M.; Sosnin, E. A.; Velichevskaya, K. Y.; Lavrent'Eva, L. V. Comparative study of UV radiation action of XeBr-excilamp and conventional low-pressure mercury lamp on bacteria. *Proc. SPIE* **2007**, *6938*, 693813.
(46) Wang, H.; Lin, C. K.; Liu, X. M.; Lin, J.; Yu, M. Monodisperse spherical core-shell-structured phosphors obtained by functionalization of silica spheres with Y_2O_3:Eu^{3+} layers for field emission displays. *Appl. Phys. Lett.* **2005**, *87* (18), 3143.
(47) Blasse, G.; Grabmaier, B. C. *Luminescent Materials*. Springer, 1994.
(48) Wang, H.; Yu, M.; Lin, C.; Liu, X.; Lin, J. Synthesis and Luminescence Properties of Monodisperse Spherical Y_2O_3:Eu^{3+}@SiO_2 Particles with Core-shell Structure. *J. Phys. Chem. C* **2007**, *111* (30), 11223−11230.
(49) Hirai, T.; Hirano, T.; Komasawa, I. Preparation of Y_2O_3:Eu^{3+} phosphor fine particles using an emulsion liquid membrane system. *J. Mater. Chem.* **2000**, *10* (10), 2306−2310.
(50) Jiang, Y. D.; Wang, Z. L.; Zhang, F. L.; Paris, H. G.; Summers, C. J. Synthesis and characterization of Y_2O_3:Eu^{3+} powder phosphor by a hydrolysis technique. *J. Mater. Res.* **1998**, *13* (10), 2950−2955.

DOI: 10.1021/acssuschemeng.7b04796
ACS Sustainable Chem. Eng. 2018, 6, 4321−4329